J Appl Electrochem (2014) 44:867–879
DOI 10.1007/s10800-014-0695-x

RESEARCH ARTICLE

Effect of process parameters of plasma electrolytic oxidation on microstructure and corrosion properties of magnesium alloys

L. Pezzato · K. Brunelli · S. Gross · M. Magrini · M. Dabalà

Received: 9 December 2013 / Accepted: 28 April 2014 / Published online: 9 May 2014

Abstract In this work, a plasma electrolytic oxidation process was applied to AZ91 and AM50 magnesium alloys and commercially pure magnesium to produce a protective surface layer. The plasma electrolytic oxidation process was carried out in an alkaline phosphate solution with a DC power supply, using relatively high current densities and short treatment times. The influence of some important process parameters such as current density, treatment time and voltage was studied. The layers were characterised by scansion electron microscopy, X-ray diffraction and X-ray photoelectron spectrometry, in order to investigate the effect of the process parameters on the microstructure and chemical composition. The corrosion resistance properties of the obtained layers were investigated by potentiodynamic anodic polarization and electrochemical impedance spectroscopy tests. The current density, applied during the treatment, influenced the morphology and the thickness of the coatings, and, consequently, the corrosion resistance. The corrosion tests evidenced that the layers obtained with plasma electrolytic process provided a good corrosion protection to the magnesium and magnesium alloys.

Keywords PEO · Magnesium alloy · Corrosion · XPS · EIS · Plasma electrolytic oxidation

L. Pezzato (✉) · K. Brunelli · M. Magrini · M. Dabalà
DII, University of Padua, Via Marzolo 9, 35131 Padua, Italy
e-mail: luca.pezzato@studenti.unipd.it

S. Gross
Dipartimento di Chimica, IENI-CNR, Via Marzolo 1, 35131 Padua, Italy

1 Introduction

In recent years the interest in magnesium alloys is increasing due to their good properties, such as low density, high strength to weight ratio, good castability, good electromagnetic shielding characteristics, high dimensional stability and suitability for recycling [1, 2]. These alloys appear very promising, especially for automotive and aerospace applications, where reducing fuel consumption and associated emission is a main goal [3]. The main problems that affect these alloys are low wear resistance and poor corrosion resistance, primarily attributed to the high chemical activity of magnesium and to the unstable imperfect natural oxide film on its surface [4, 5]. Surface treatments such as anodizing, conversion coating, plating, vapour deposition, polymer coatings, plasma electrolytic oxidation are the most common ways to improve the corrosion resistance of these materials. Among these, plasma electrolytic oxidation (PEO) is a newly developed but very promising process that can enhance the corrosion and wear resistance by producing a relatively thick, dense and hard oxide coating on magnesium alloys. The PEO process seems to be a good choice to replace conventional anodic process due to two fundamental advantages: (1) it is an environmental friendly process, because it involves the use of diluted alkaline solutions as electrolyte in place of conventional chromic acid anodizing or hard acid anodizing; (2) the coatings obtained with PEO exhibit improved surface performances in terms of hardness, wear protection and corrosion resistance compared with traditional anodized layers [6, 7]. The PEO of metals is a complex process that combines oxide film formation, dissolution and dielectric breakdown and it is developed from the traditional anodic oxidation: the sample (anode) is immersed in an electrolyte and the tank is the cathode, working with

higher voltages and current densities [8, 9]. Due to the high voltage (that has to be above the dielectric breakdown potential of the oxide layer) persistent anodic micro-discharges are formed on the surface during the PEO treatment. These short-lived micro-discharges are the key factors of the process; they move randomly over the processed surface and produce the growth of an oxide ceramic coating [10]. The corrosion behaviour of magnesium and magnesium alloys treated with PEO strongly depends on some important process parameters: current density, voltage, treatment time and electrolyte composition [11]. In literature, several works about PEO of magnesium alloys can be found. In particular, the effects of additives in the electrolyte and of the operating conditions were studied [12–18]. In previous works PEO processes were performed mainly using low current densities (0.01–0.1 A cm^{-2}) and long treatment times (5–60 min) [19–22].

In this paper, a PEO process was performed on pure magnesium and magnesium alloys (AM50 and AZ91). The effects of the current density and treatment time on the morphology, thickness, chemical composition and corrosion resistance of the coatings, were investigated. In respect to previous studies, it was chosen to work with higher current densities (0.1–0.45 A cm^{-2}) and shorter treatment times (20–60 s). An alkaline solution containing both phosphates and fluorides was used as electrolyte.

2 Experimental

Samples of commercially pure magnesium, AZ91 and AM50 alloy were used as substrate for PEO coatings. The nominal composition of the alloys is reported in Table 1. Before PEO treatment, the samples were polished following standard metallographic techniques and then degreased using acetone in ultrasound. The PEO electrolyte was constituted by an aqueous alkaline solution with 100 g L^{-1} of $Na_5P_3O_{10}$, 40 g L^{-1} of NaOH and 42 g L^{-1} of NaF. The plasma electrolytic oxidation process was carried out using a TDK-Lambda DC power supply of 300 V/8A capacity. During the treatment, the sample worked as anode and the cathode was a stainless steel crucible that contained the electrolyte. The treatments were performed maintaining the current constant, letting the potential free to vary.

The formation of the oxide ceramic layer was obtained using: (1) different current densities (0.1–0.2–0.25–0.35–0.45 A cm^{-2}) with the same treatment time (60 s); (2) the same current density (0.25 or 0.45 A cm^{-2}) with different treatment times (20–40–80 s). The initial and final polarization voltage, achieved during the experiment at the different current density values, are reported in Table 2. After the treatment, the samples were washed with deionised water and ethanol and dried with compressed air. The cross-sections of the treated samples were cut and mounted in epoxy resin and polished with standard metallographic technique. Both the surface and the cross-section of treated samples were examined with a Cambridge Stereoscan 440 scanning electron microscope, equipped with a Philips PV9800 EDS, in order to evaluate the morphological features, the thickness of the coating and the elemental composition. The phase analysis was carried out with a Siemens D500 X-ray diffractometer using Cu Kα radiation. XPS spectra were run on a Perkin-Elmer Φ5600ci spectrometer using standard Al radiation (1486.6 eV) working at 250 W. The working pressure was $<5 \times 10^{-8}$ Pa. The spectrometer was calibrated by assuming the binding energy (BE) of the $Au4f_{7/2}$ line at 83.9 eV with respect to the Fermi level. The SD for the BE values was 0.15 eV. The reported BE were corrected for the charging effects, assigning, in the outer layers where contamination carbon is still present, to the C1s line of carbon the BE value of 284.6 eV [23]. Survey scans (187.85 pass energy, 1 eV/step, 25 ms per step) were obtained

Table 2 Final and initial polarization voltages achieved for different samples under various current density values in the electrolyte 100 g L^{-1} of $Na_5P_3O_{10}$, 40 g L^{-1} of NaOH and 42 g L^{-1} of NaF

	Initial potential (V)	Final potential (V)
Commercially pure magnesium treated at 0.1 A cm^{-2}	55	58
Commercially pure magnesium treated at 0.25 A cm^{-2}	55	65
Commercially pure magnesium treated at 0.35 A cm^{-2}	55	75
Commercially pure magnesium treated at 0.45 A cm^{-2}	55	80
AZ91 alloy treated at 0.1 A cm^{-2}	50	60
AZ91 alloy treated at 0.25 A cm^{-2}	50	70
AZ91 alloy treated at 0.35 A cm^{-2}	50	90
AZ91 alloy treated at 0.45 A cm^{-2}	50	100
AM50 alloy treated at 0.1 A cm^{-2}	55	65
AM50 alloy treated at 0.25 A cm^{-2}	55	70
AM50 alloy treated at 0.35 A cm^{-2}	55	85
AM50 alloy treated at 0.45 A cm^{-2}	55	95

Table 1 Chemical composition of the alloys

Alloy	Al (%)	Zn (%)	Mn (%)	Si (%)	Fe (%)	Cu (%)	Ni (%)	Other (%)
AM50	5.0	<0.22	0.25	<0.10	<0.005	<0.010	<0.002	<0.030
AZ91	9.0	0.65	0.15	<0.10	<0.005	<0.010	<0.002	<0.030

in the 0–1300 eV range. The atomic composition, after a Shirley type background subtraction [24], was evaluated using sensitivity factors supplied by Perkin [25]. The assignments of the peaks were carried out by using the values reported in the reference handbook [25], in the NIST XPS Database [26, 27] and in the references reported in [28–31].

The corrosion resistance of the coating was analyzed by anodic polarization tests and electrochemical impedance spectroscopy (EIS) at ambient temperature. The anodic polarization tests were performed in a solution containing 0.1 M Na_2SO_4 and 0.05 M NaCl, with an AMEL 7060 Potentiostat, using a saturated calomel electrode as reference electrode (SCE) and a platinum electrode as counter electrode with a scan rate of 1 mV s^{-1}. The EIS measurements were carried out in the previous described solution at the value of the open circuit potential and in a frequency range between 10^5 and 10^{-2} Hz with a perturbation amplitude of 5 mV. The impedance measurements were recorded with a Solartron Schlumberger 1255 FRA Spectrometer coupled with a EG&G 273A Potentiostat and the ZView software was used for the fitting of impedance spectra.

3 Results and discussion

During the PEO process a large number of sparks/microdischarges occurred on the surface of the samples; the number of these sparks increased with the current density and the treatment time. The treatments were performed working at constant current density, and monitoring the potential. A potential increase was observed during the process of 60 s, and depended quantitatively on the current density applied. In fact, for low current densities a potential increase of about 10–20 V was measured, whereas the increase was more important (about 40–50 V) for the treatments carried out at high current densities (see Table 2).

The morphology of the surface layers, on commercially pure magnesium, obtained with PEO process at different current densities for the same time (60 s), are shown in Fig. 1. The surfaces of all samples showed numerous craters and pores and the number of pores decreased with the increase of the current density applied during the treatment. In detail, passing from the sample treated at 0.1 A cm^{-2} to the sample treated at 0.45 A cm^{-2}, there was a significant

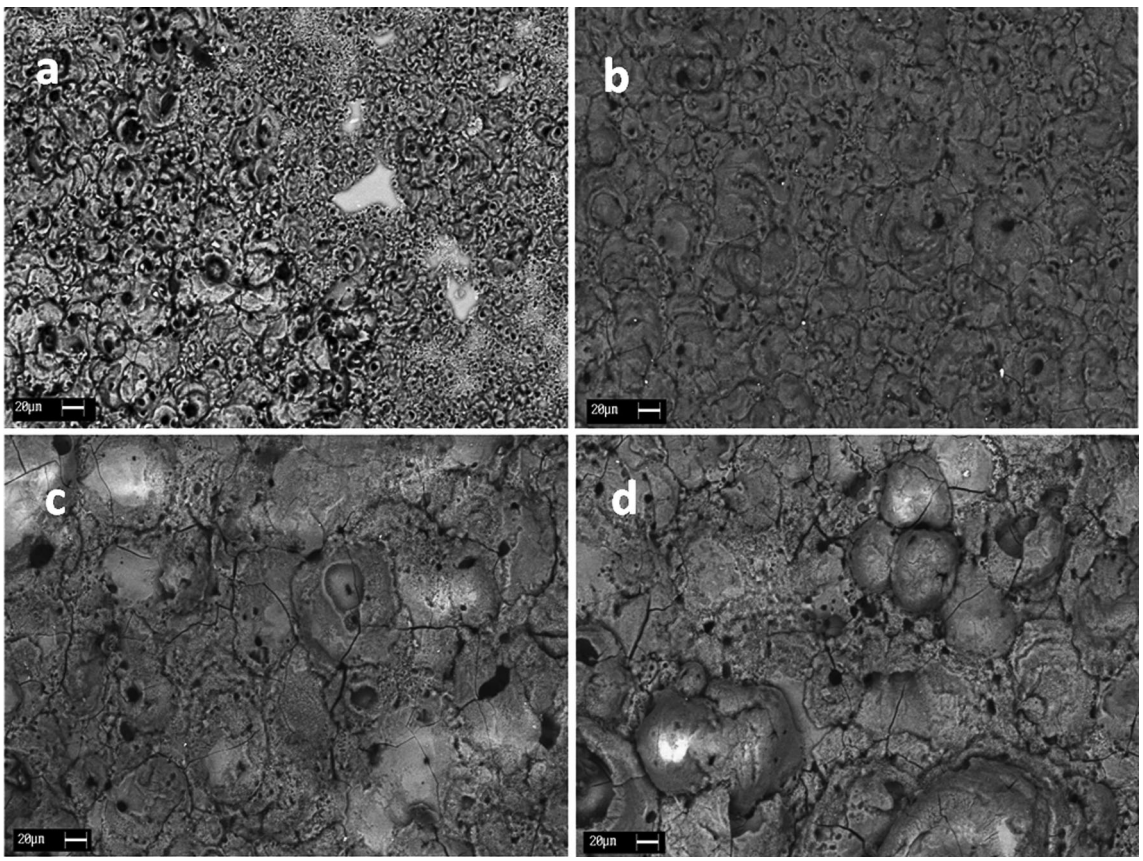

Fig. 1 Scanning electron micrographs (backscattered electrons, 650×) of the surface of PEO coatings formed on commercially pure magnesium. All the samples were treated for 60 s at 0, 1 A cm^{-2} (**a**), 0.25 A cm^{-2} (**b**), 0.35 A cm^{-2} (**c**) and 0.45 A cm^{-2} (**d**)

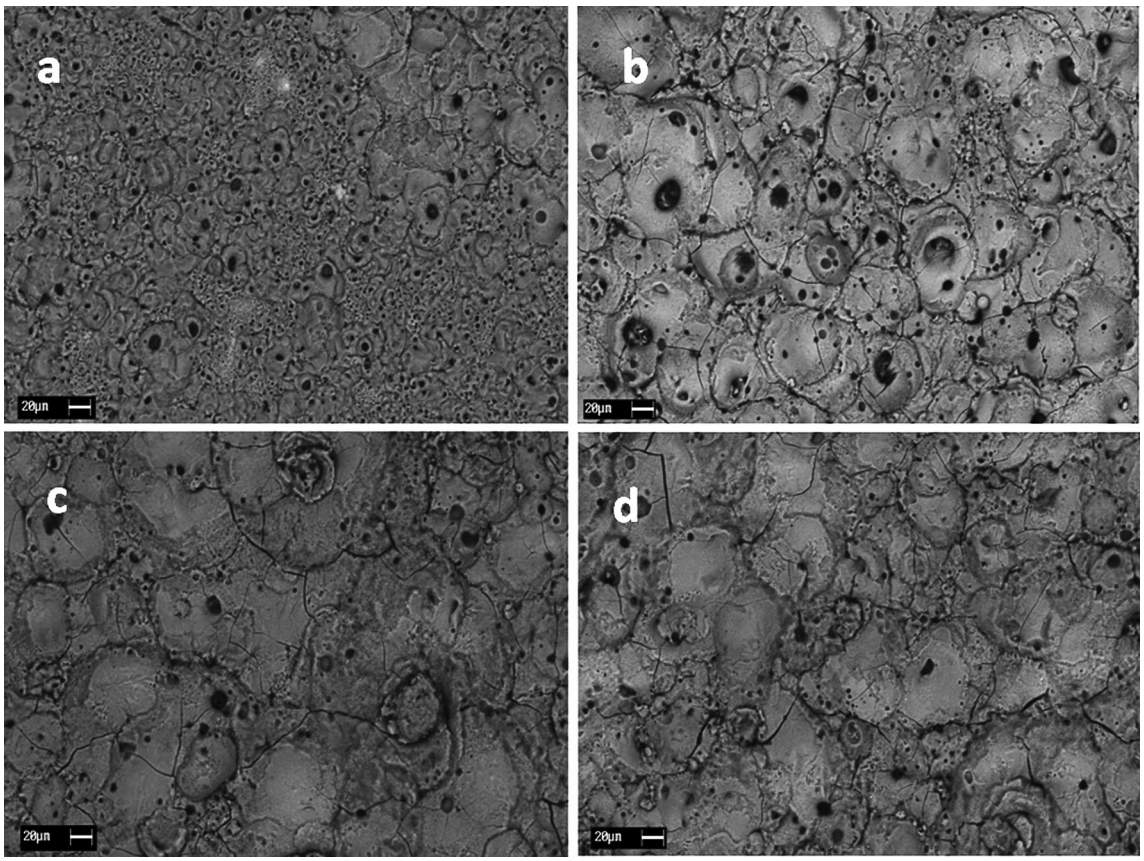

Fig. 2 Scanning electron micrographs (backscattered electrons, 650×) of the surface of PEO coatings formed on AZ91 magnesium alloy. All the samples were treated for 60 s at 0.1 A cm^{-2} (**a**), 0.25 A cm^{-2} (**b**), 0.35 A cm^{-2} (**c**) and 0.45 A cm^{-2} (**d**)

reduction in the number of pores. In the sample treated at the lowest current density (0.1 A cm^{-2}) also some zones were visible that were not completely coated during the PEO treatment, and indeed, from EDS analysis, they resulted to be constituted only by Mg. Moreover, a large number of micro-cracks were observed, probably caused by residual stress resulting from rapid quenching of the molten materials at the solid/electrolyte interface, during the plasma discharges.

The layers obtained by PEO process, at different current densities for the same time (60 s), on the surface of AZ91 and AM50 alloys showed the same morphology seen on the surface of pure magnesium: a decreasing porosity occurred with the increase of the current density applied in the treatment (Figs. 2, 3).

The cross-section images of the PEO coated sample for pure magnesium at different current densities are presented in Fig. 4. An increase in the thickness of the surface layer passing from the sample treated at 0.1 A cm^{-2} (6 µm thick) to the one treated at 0.35 A cm^{-2} (47 µm thick) was observed. The detachment of the layer and the presence of cracks could be due to the damage occurred during the sample preparation (cutting and grinding). The thickness of the oxide layer in the sample obtained at 0.45 A cm^{-2} was lower than the one of the sample treated at 0.35 A cm^{-2} (30 vs 47 µm, respectively), but the last resulted more continuous and homogenous.

In the cross-section images of the PEO coated samples of AZ91 and AM50 alloy a continuous surface layer was observed, except for AZ91 treated with the current density at 0.1 A cm^{-2}, where only isolated islands were visible. The thicker layer grew with the current applied in the treatment: 2 and 7 µm at 0.1 A cm^{-2}, 30 and 17 µm at 0.35 A cm^{-2}, and 60 and 55 µm at 0.45 A cm^{-2}, for AZ91 and AM50 respectively (Figs. 5, 6). Therefore, from SEM analysis, it resulted that working at high current density with relatively short treatment times allowed the formation of a thick oxide layer.

The chemical composition and the phase analysis of the layers were investigated by EDS and XRD, respectively. EDS analysis, carried out on the surface, revealed that the composition of the coating was not significantly influenced by the current density applied during the treatment, and the EDS spectra of the various samples were substantially the same. The surface of the coating formed on commercially pure Mg was principally composed by O, Na, Mg, P and F,

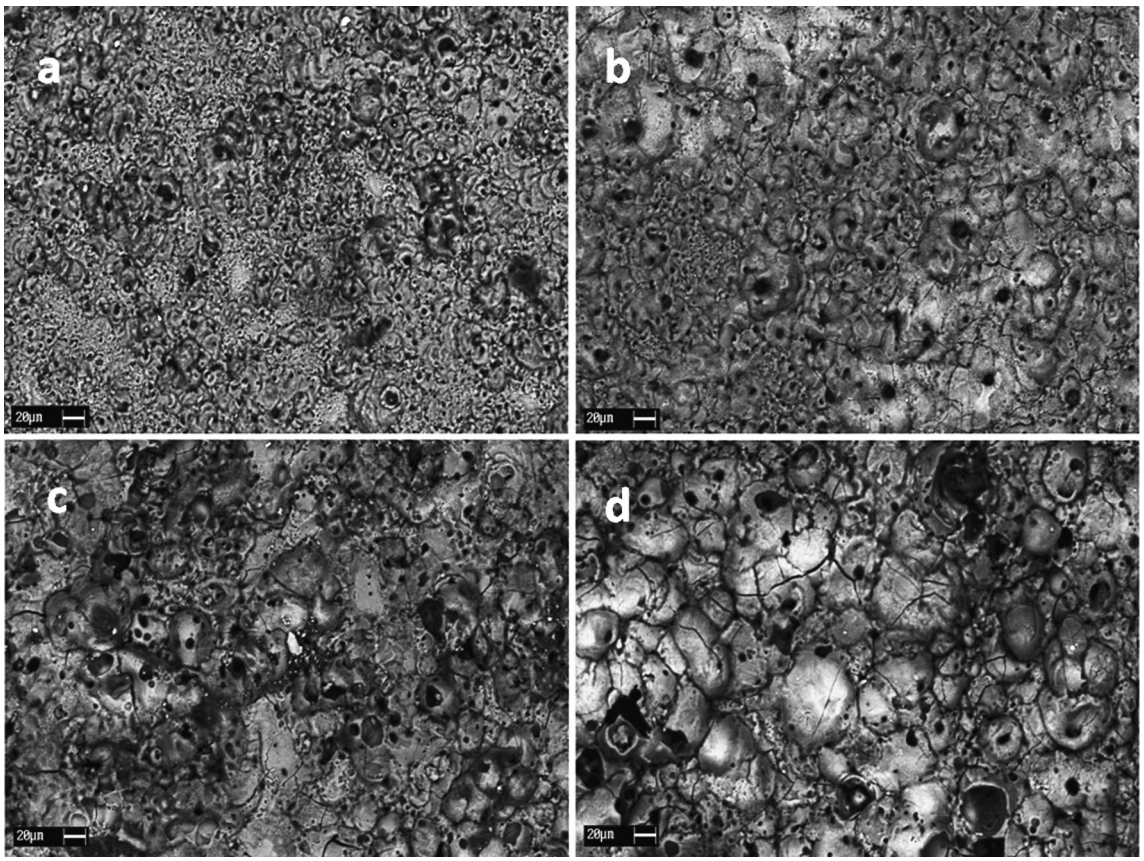

Fig. 3 Scanning electron micrographs (backscattered electrons, 650×) of the surface of PEO coatings formed on AM50 magnesium alloy. All the samples were treated for 60 s at 0.1 A cm^{-2} (**a**), 0.25 A cm^{-2} (**b**), 0.35 A cm^{-2} (**c**) and 0.45 A cm^{-2} (**d**)

whereas in AM50 and AZ91 alloys, besides the elements cited, also Al was registered, due to its presence in the alloy. The quantitative results of EDS analysis of the cross-sectioned surface layers (excluding oxygen that forms with the other elements oxides and phosphates) are reported in Table 3. EDS elemental profiles were performed among the cross-section of the samples in order to evaluate the composition of the layer along the thickness. The elemental profile carried out in the layer of AZ91, obtained at 0.45 A cm^{-2} for 60 s, showed that no variations in elemental concentration along the cross-section of the coating was registered, except for sodium, whose concentration increased near the surface (Fig. 7). In addition, a slight increase of F, in proximity of the surface was observed. The tests on AM50 and commercially pure magnesium gave the same results obtained for AZ91 alloy with an enrichment of sodium and F (less marked for this last element) in the portion of the layer near the surface.

XRD analysis was performed only on the samples of pure commercially magnesium and of AZ91 and AM50 alloys treated at 0.45 A cm^{-2} for 60 s. The patterns are presented in Fig. 8. In all patterns the presence of the Mg peak was observed, due to the reflection from the substrate. The peaks of magnesium phosphate $Mg(PO_3)_2$, magnesium oxide MgO, and sodium fluoride NaF, were visible in all the alloys. In AM50 and AZ91 alloys also the presence of aluminium oxides (Al_2O_3) and mixed aluminium-magnesium oxides ($MgAl_2O_4$) were detected. The composition of the layer was clearly connected with the electrolyte used in this PEO process, constituted by an alkaline solution of sodium phosphate and sodium fluoride. Therefore, in the coating phosphates and fluorides could be found. The presence of NaF could be due to the adsorption effect on the surface. As a matter of fact, from EDS analysis an enrichment of these two elements resulted near the surface.

In order to obtain information about the composition and the state of oxidation of the elements in the ceramic oxide layer obtained with PEO process, XPS analysis (without sputtering) were performed on the sample of pure commercial Mg treated at 0.45 A cm^{-2}. The survey spectrum of the sample is shown in Fig. 9. From the collected spectrum of the main photoelectron lines (C1s, O1, F1s, Na1s, Mg1s and P2p), the atomic percentages of the elements present in the external surface of the coating were calculated. The layer resulted to be principally constituted by O, Mg, F, P and Na, in agreement with the previous

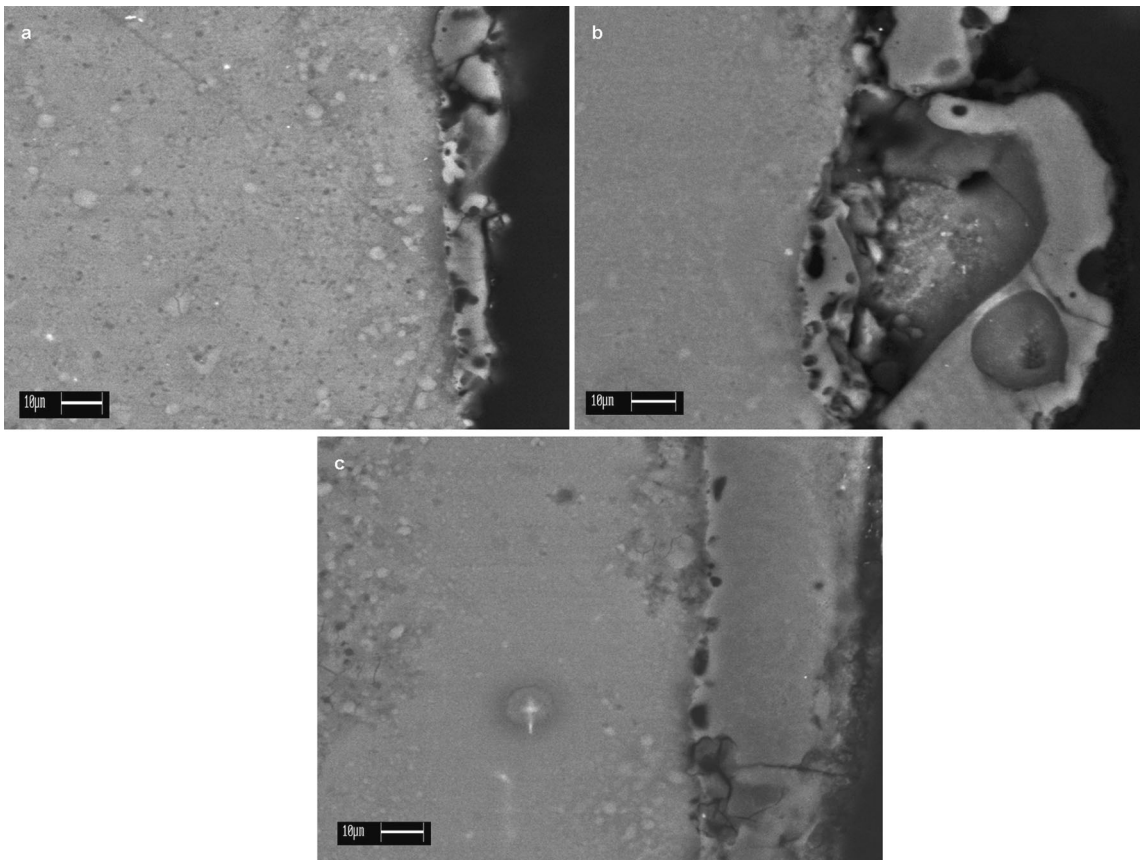

Fig. 4 Scanning electron micrographs (backscattered electrons, 750×) of the cross section of PEO coatings formed on commercially pure magnesium samples treated for 60 s at 0.1 A cm^{-2} (**a**), 0.35 A cm^{-2} (**b**) and 0.45 A cm^{-2} (**c**)

analysis. The presence of C is attributable to ambient contamination. The peak of Mg2s binding energy of 89.1 eV and the peak of Mg2p binding energy of 50.4 eV were assigned to the presence of MgO [25, 26]. The peak of Na1s binding energy of 1071.6 eV was attributed to the NaF compound [26] and the peaks of P2s and P2p binding energy 191.0 and 133.9 eV, respectively, were associated to the presence of $Mg_3(PO_4)_2$ [32]. The presence of NaF is probably due to the adsorption effect on the surface, in agreement with EDS and XRD analysis.

3.1 Corrosion behaviour

To study the corrosion properties of the layers produced by the PEO process, potentiodynamic anodic polarization and EIS test were performed in a solution containing both sulphates and chlorides (0.1 M Na_2SO_4 and 0.05 M NaCl).

3.1.1 Potentiodynamic polarization tests

The anodic polarization plots for commercially pure magnesium treated with different current densities for 60 s are reported in Fig. 10a and the corrosion current densities i_{corr} and corrosion potentials E_{corr} for the different treatments are reported in Table 4. The corrosion resistance of the PEO treated samples was significantly improved compared with the untreated one. As a matter of fact, a decrease in the current density and an increase in the corrosion potential were observed. In particular, the untreated sample and the one treated at 0.45 A cm^{-2}, the decrease of i_{corr} was higher than one order of magnitude. In terms of corrosion potential, in comparison with the untreated sampled, there was a slight decrease for the sample treated at 0.1 A cm^{-2}, whereas an increase for all the other treated samples was registered, with ennoblement of 0.14 V for the sample treated at 0.45 A cm^{-2}. The better corrosion properties of the samples treated with higher current densities can be directly colligated with the thicker layer and the reduction of the porosity on the surface, that both were previously observed by SEM for high current densities applied in the treatment.

The anodic polarization plot and the resulting data for AM50 alloy treated at different current densities for 60 s are reported in Fig. 10b and Table 4. Also for this alloy the

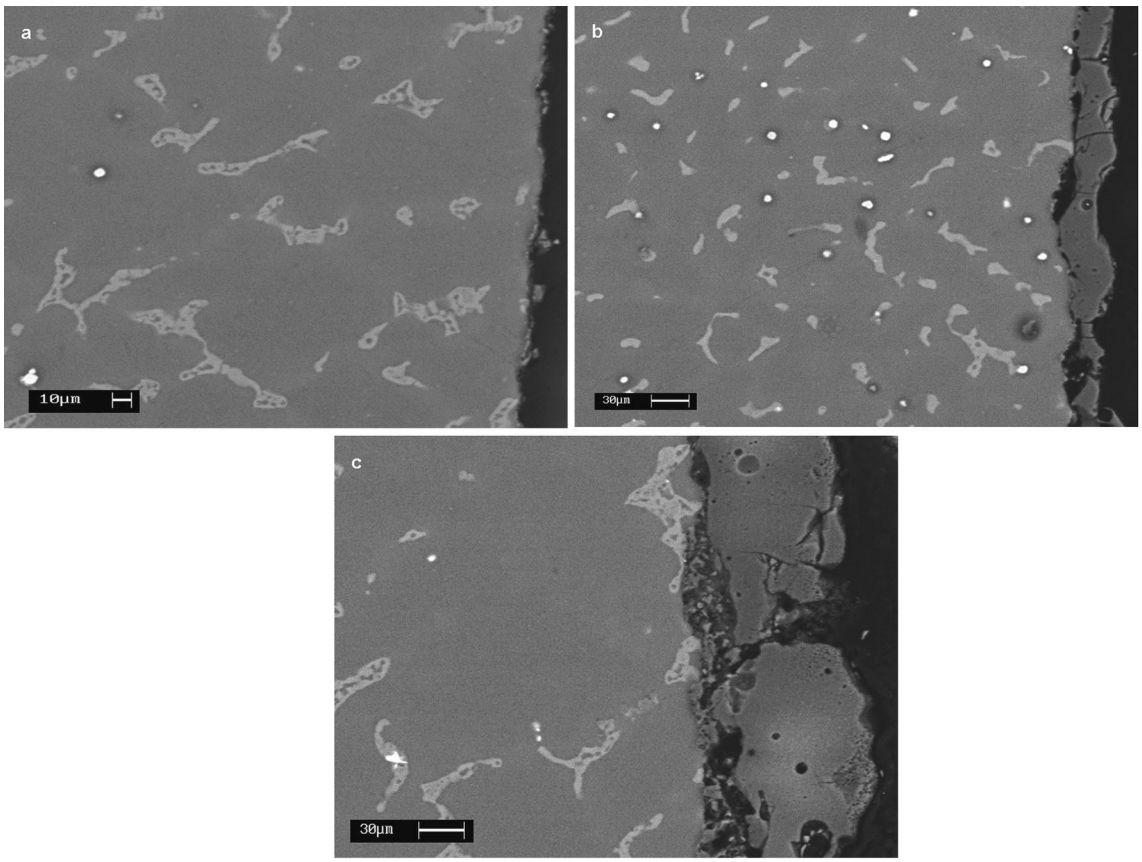

Fig. 5 Scanning electron micrographs (backscattered electrons, 750×) of the cross section of PEO coatings formed on AZ91 magnesium alloy samples treated for 60 s at 0.1 A cm^{-2} (**a**), 0.35 A cm^{-2} (**b**) and 0.45 A cm^{-2} (**c**)

values of E_{corr} indicated that PEO treatment caused an increase in the corrosion potential in comparison with the untreated sample and that this effect was more evident with high current densities applied (an ennoblement about 0.18 V for the sample treated at 0.45 A cm^{-2} was observed). For AM50 alloy it can be observed that the values of i_{corr} of the treated samples were more or less the same and one order of magnitude lower than the one of the untreated sample, indicating the improvement in corrosion resistance due to PEO treatment. In this alloy, a passivation phenomenon can be observed for the sample treated at 0.1 A cm^{-2}. For AZ91 the anodic polarization plot and the values of E_{corr} and i_{corr} are reported in Fig. 10c and Table 4. As it was observed for the previous materials, the PEO treatments caused an ennoblement in the corrosion potential and it increased the current density applied in the treatment. An ennoblement of 0.42 V was measured for the sample treated at 0.45 A cm^{-2}. The values of i_{corr} for AZ91 alloy for the samples treated at 0.25, 0.35 and 0.45 A cm^{-2} are more or less the same and one order of magnitude lower than the values of the untreated sample and the sample treated at 0.1 A cm^{-2}. Also for AZ91 alloy, the samples treated at 0.35 and 0.45 A cm^{-2} showed a passivation phenomenon. Potentiodynamic polarization tests were also performed on samples treated with the same current density (0.25 or 0.45 A cm^{-2}) but with different treatment times (20, 40, 60, 80 s). These tests were carried out to evaluate the effect of the treatment time on the corrosion properties of the coatings. The results of this tests for AZ91 alloy treated at 0.25 A cm^{-2} for various treatment times were reported in Fig. 11, where the sample treated for 60 s showed the better corrosion resistance, even if its values of i_{corr} and E_{corr} were very similar to the ones of the samples treated for 40 and 80 s. Only the sample treated for 20 s presented values of i_{corr} and E_{corr} significantly lower than the others. A similar behaviour was found for AZ91 alloy treated at 0.45 A cm^{-2} and for commercially pure magnesium and AM50 alloy at both current densities.

These results showed that increasing the treatment time causes only a slight improvement in the corrosion resistance of the samples. Therefore, the effect of the treatment time was quantitatively less important than the effect of the current density. Increasing the current density applied in

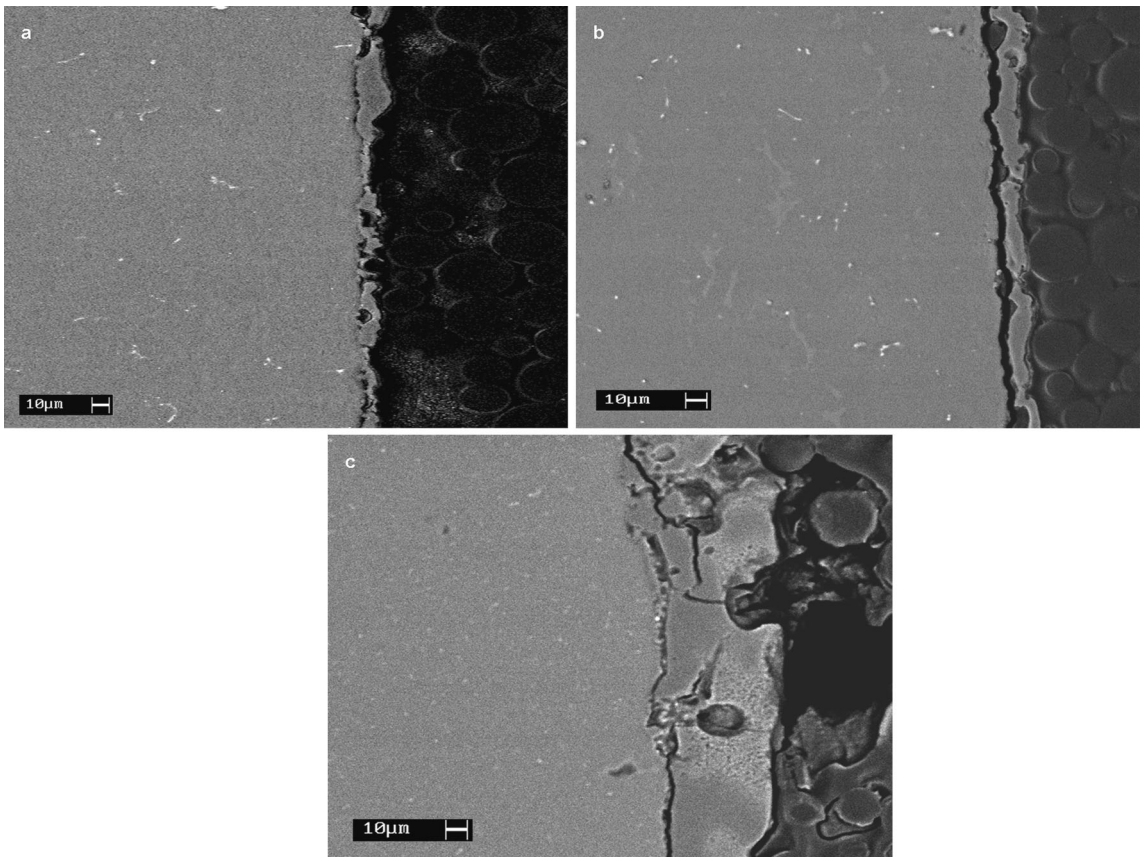

Fig. 6 Scanning electron micrographs (backscattered electrons, 750×) of the cross section of PEO coatings formed on AM50 magnesium alloy samples treated for 60 s at 0.1 A cm^{-2} (**a**), 0.35 A cm^{-2} (**b**) and 0.45 A cm^{-2} (**c**)

Table 3 Quantitative results (wt%) of EDS analysis of the cross-sectioned surface layers

Alloy	Mg (%)	P (%)	Na (%)	Al (%)	F (%)
Pure magnesium	60.51	21.41	9.63	–	8.44
AZ91	47.44	31.17	7.64	7.28	6.46
AM50	43.16	43.81	7.72	2.27	3.05

the PEO treatment caused a good improvement in the corrosion resistance with ennoblement in the corrosion potential and a decrease of more than one order of magnitude in the current density.

3.1.2 Electrochemical impedance spectroscopy

To better understand the corrosion characteristics of the PEO coated specimens, EIS tests were performed on the alloys treated at 0.1 and 0.45 A cm^{-2} for 60 s. The data coming from EIS tests were fitted for quantitative evaluation with the software Z-view using the equivalent circuit, shown in Fig. 12. A good fitting quality was obtained, as it

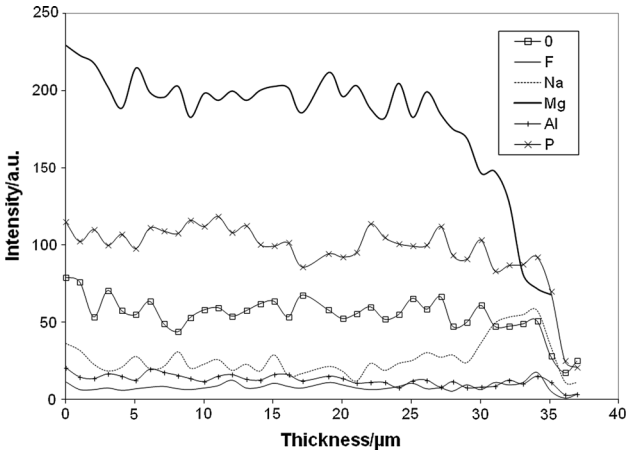

Fig. 7 EDAX line microanalysis for the cross section of an AM50 sample treated at 0.35 A cm^{-2} for 60 s. The plot goes from the interface metal-coating to the surface

can be observed in Fig. 13, where continuous lines represent simulation data (Chi squared values varied between 0.005 and 0.05). In the equivalent circuit, the value of R_1 represented the resistance of the solution; the polarization

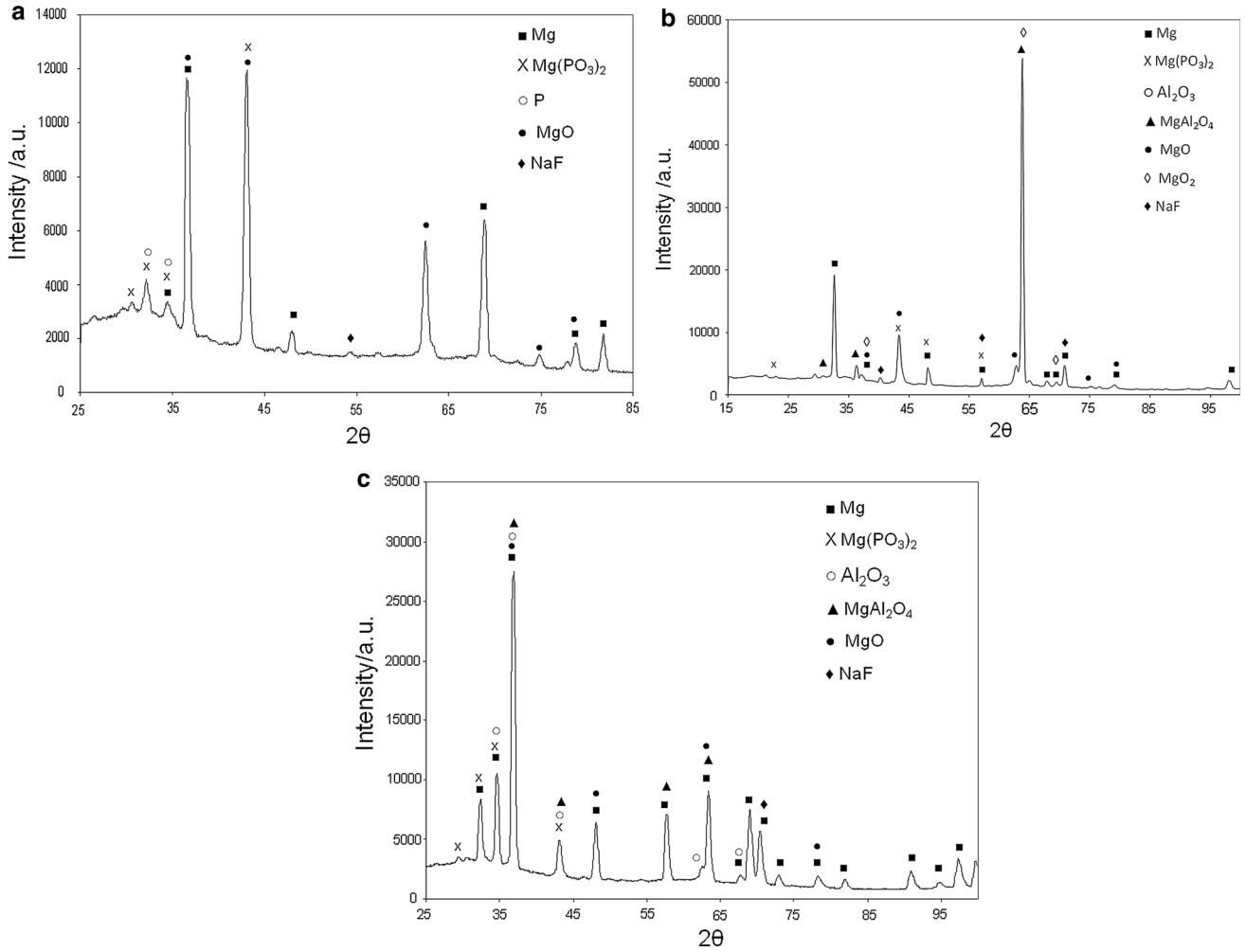

Fig. 8 X-ray diffraction patterns for **a** commercially pure magnesium; **b** AZ91 alloy and **c** AM50 alloy PEO coated at 0.45 A cm^{-2} for 60 s

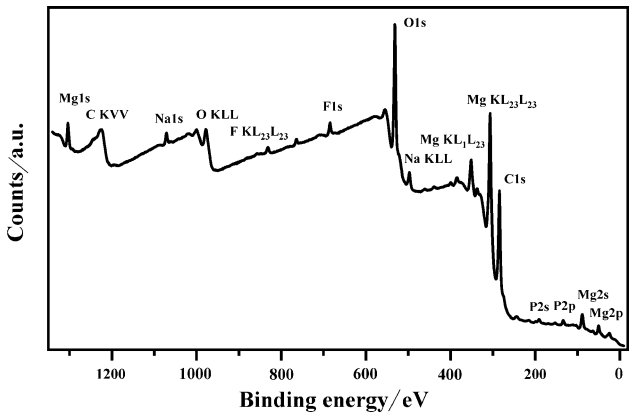

Fig. 9 XPS survey spectra for commercially pure magnesium PEO coated at 0.45 A cm^{-2} for 60 s

resistance R_2 is a measure of corrosion resistance of the material in the environment; a constant phase element (CPE) was used in the equivalent circuit instead of a capacitance because often the measured capacitance is not ideal. The impedance representation of CPE is given by:

$$Z(CPE) = 1/[Q(j\omega)^n] \quad (1)$$

Q is a constant phase element and ω is the angular frequency. The number n is an empirical exponent, which can vary between 1 for a perfect capacitor and 0 for a perfect resistor. A value of n less than one would represent a somewhat capacitor and it is generally thought to arise from the presence of heterogeneities both laterally and within the depth of the coating. If the values of the exponent n are approximately one, Q can be said to behave similar to a pure capacitor and the Eq. 2 is valid that defines the capacitance of the parallel plate capacitor:

$$C = \varepsilon_0 \varepsilon A / d_{ox} \quad (2)$$

where C is the capacitance, ε_0 is the permittivity of vacuum, ε is the dielectric constant, A the effective area and

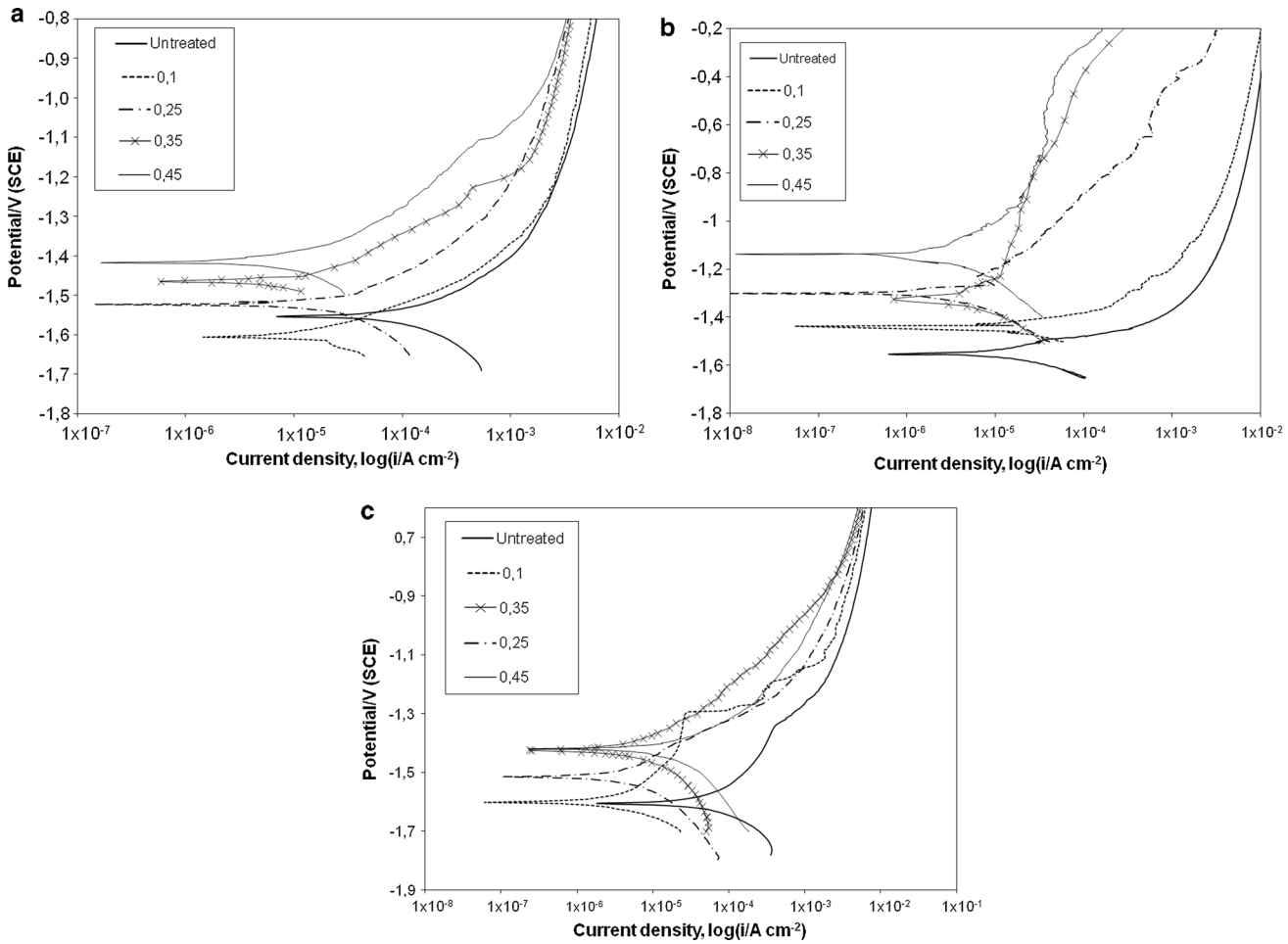

Fig. 10 Potentiodynamic polarisation plots for **a** commercially pure magnesium; **b** AM50 alloy and **c** AZ91 alloy PEO coated at different current densities for 60 s (test electrolyte: 0.1 M Na_2SO_4 + 0.05 M NaCl)

Table 4 Results of the anodic polarization test in 0.1 M Na_2SO_4 + 0.05 M NaCl solution for samples treated at different current densities for 60 s

	i_{corr} (A cm^{-2})	E_{corr} (V)
Commercially pure magnesium untreated sample	1×10^{-4}	−1.55
Commercially pure magnesium treated at 0.1 A cm^{-2}	3×10^{-5}	−1.6
Commercially pure magnesium treated at 0.25 A cm^{-2}	2×10^{-5}	−1.52
Commercially pure magnesium treated at 0.35 A cm^{-2}	5×10^{-6}	−1.46
Commercially pure magnesium treated at 0.45 A cm^{-2}	5×10^{-6}	−1.41
AZ91 alloy untreated sample	2.6×10^{-5}	−1.56
AZ91 alloy treated at 0.1 A cm^{-2}	1×10^{-5}	−1.44
AZ91 alloy treated at 0.25 A cm^{-2}	4×10^{-6}	−1.3
AZ91 alloy treated at 0.35 A cm^{-2}	3×10^{-6}	−1.34
AZ91 alloy treated at 0.45 A cm^{-2}	2×10^{-6}	−1.14
AM50 alloy untreated sample	7×10^{-5}	−1.6
AM50 alloy treated at 0.1 A cm^{-2}	4×10^{-6}	−1.6
AM50 alloy treated at 0.25 A cm^{-2}	3×10^{-6}	−1.5
AM50 alloy treated at 0.35 A cm^{-2}	4×10^{-6}	−1.42
AM50 alloy treated at 0.45 A cm^{-2}	5×10^{-6}	−1.42

The values of E_{corr} are given versus SCE

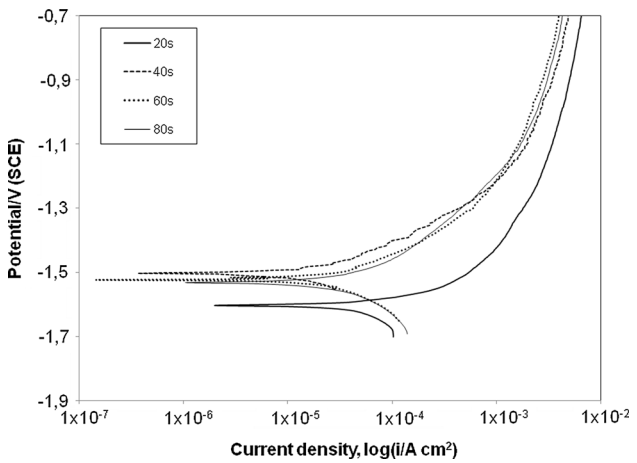

Fig. 11 Potentiodynamic polarisation plot for AZ91 alloy PEO coated at 0.25 A cm^{-2} and different treatment times (test electrolyte: 0.1 M Na_2SO_4 + 0.05 M NaCl)

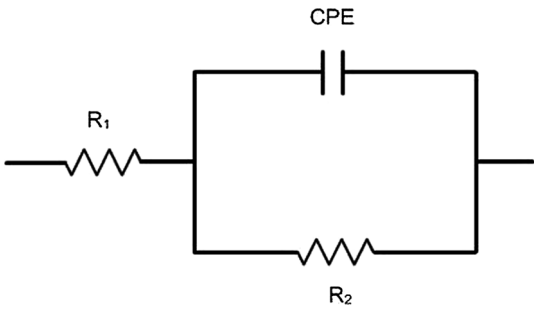

Fig. 12 Equivalent circuit employed for curve fitting

d the distance of the plates that can be used to estimate the thickness of the coating.

For the samples of commercially pure magnesium, the Nyquist impedance plot and the fitting results are reported in Fig. 13a and Table 5. Increasing the current density of the PEO process, induced also an increase in the value of R_2, the polarization resistance, which is inversely proportional to i_{corr}. In detail, the R_2 of the sample treated at 0.45 A cm^{-2} was one order of magnitude higher than the one of the untreated sample. Moreover, a decrease in the value of Q can be observed passing from the untreated

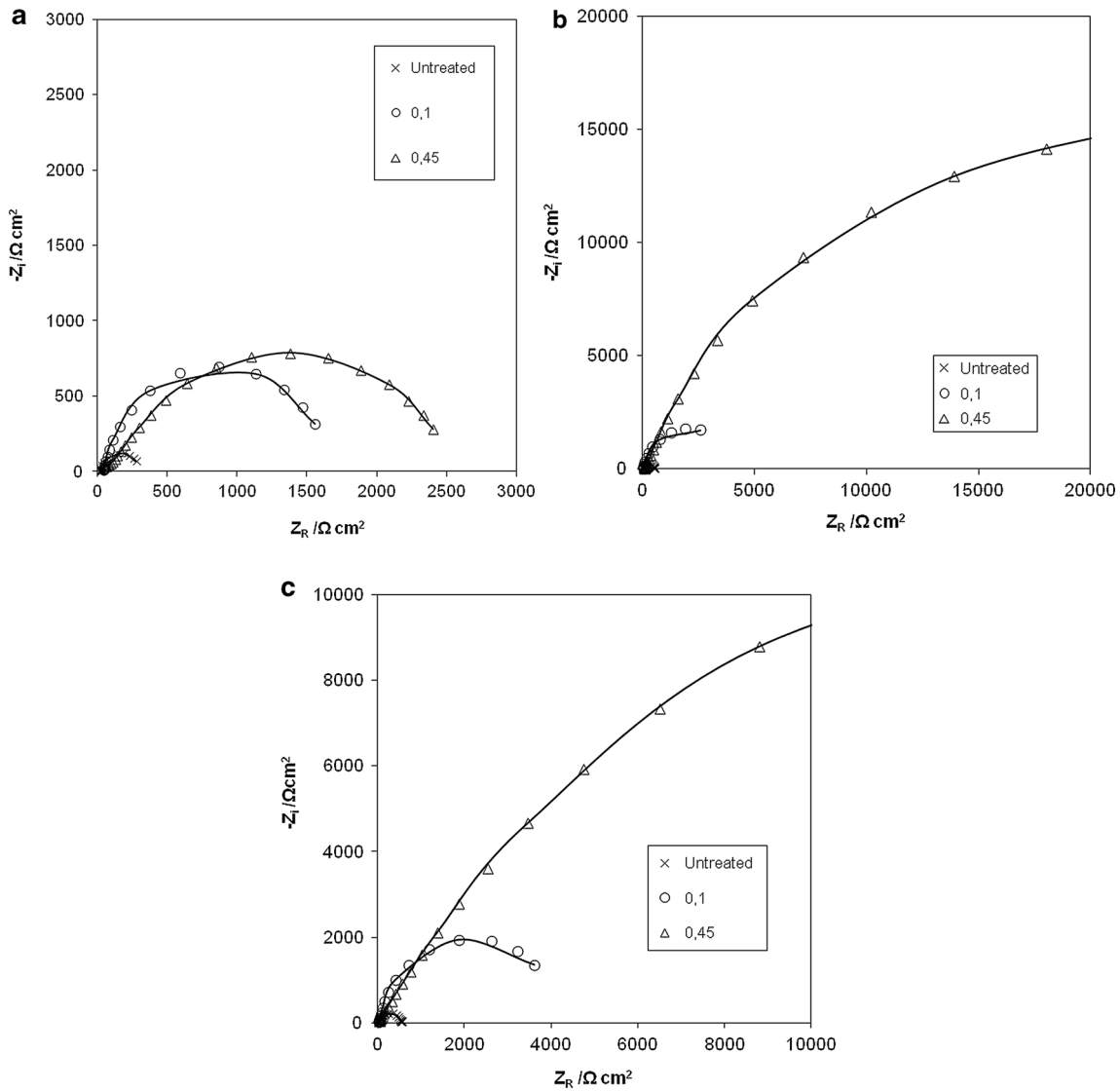

Fig. 13 Nyquist plots for **a** commercially pure magnesium; **b** AZ91 alloy and **c** AM50 alloy PEO coated at different current densities for 60 s (test electrolyte: 0.1 M Na_2SO_4 + 0.05 M NaCl). *Continuous lines* represent simulation data and points experimental data

Table 5 Equivalent circuit data for samples treated at different current densities for 60 s

	R_1 (Ω cm^2)	Q (F Hz^{1-n})	n	R_2 (Ω cm^2)
Commercially pure magnesium untreated sample	25.46	1.71×10^{-5}	0.93	274
Commercially pure magnesium treated at 0.1 A cm^{-2}	26.12	6.21×10^{-6}	0.74	1,937
Commercially pure magnesium treated at 0.45 A cm^{-2}	26.13	3.24×10^{-6}	0.74	2,667
AZ91 alloy untreated sample	23.36	1.72×10^{-5}	0.88	519
AZ91 alloy treated at 0.1 A cm^{-2}	25.75	3.49×10^{-6}	0.86	4,473
AZ91 alloy treated at 0.45 A cm^{-2}	25.48	1.86×10^{-6}	0.84	20,639
AM50 alloy untreated sample	25.32	9.83×10^{-5}	0.78	632
AM50 alloy treated at 0.1 A cm^{-2}	23.18	2.14×10^{-6}	0.81	4993
AM50 alloy treated at 0.45 A cm^{-2}	25.12	4.22×10^{-6}	0.76	40035

sample to the sample treated at 0.45 A cm^{-2}. From Eq. 2, the lower value of Q, obtained for the samples treated at high current density, can be correlated with an increase in the thickness, in agreement with the results from SEM observation.

The Nyquist impedance plots and the results of the data fitting, for AZ91 alloy, are reported in Fig. 13b and in Table 5, respectively. Similarly to the results obtained for pure commercially magnesium, a decrease in the values of Q and an increase in the values of R_2 were found for the samples with PEO treatment, in comparison with the untreated sample, suggesting the presence of a thicker and more protective layer. It should be noted, that the value of R_2 for the sample treated at 0.45 A cm^{-2} was two order of magnitude higher than the one of the untreated sample, whereas for commercially pure magnesium, at the same operative conditions, this value was only one order of magnitude higher than the one of the untreated sample. The Nyquist impedance plots and the results of fitting of the data for AM50 alloy are reported in Fig. 13c and Table 5, where a behaviour very similar to AZ91 alloy can be observed. These results evidenced that the PEO process caused an enhancement in the corrosion resistance of both pure magnesium and magnesium alloys, but the improvement was more evident for magnesium alloys, in agreement with the results coming from anodic polarization tests.

4 Conclusions

The PEO process performed, using as electrolyte an aqueous alkaline solution containing phosphates and fluorides, produced on magnesium and magnesium alloy a thick ceramic layer, principally constituted by oxides, phosphates and fluorides. Working with high current densities and very short times allowed the formation of a thick surface layer. The current density applied during the treatment influenced the morphology, the thickness, and the corrosion properties of the layers but not the compisiton. The increase of the current density caused a reduction in the number of pores on the surface and an increase in the thickness of the coating. The effect of the treatment time was quantitatively less important than the one of the current density. PEO coated samples exhibited improved corrosion properties as evidenced by potentiodynamic anodic polarization tests and EIS tests, in comparison with untreated samples. EIS tests in particular evidenced that both magnesium and magnesium alloys showed an enhancement in the corrosion resistance due to the PEO treatment, but the improvement was higher for magnesium alloys compared with the one of commercially pure magnesium.

References

1. Liang J, Bala-Srinivasan P, Blawert C, Störmer M, Dietzel W (2009) Electrochemical corrosion behaviour of plasma electrolytic oxidation coatings on AM50 magnesium alloy formed in silicate and phosphate based electrolytes. Electrochim Acta 54:3842–3850
2. Mordike BL, Ebert T (2001) Magnesium properties—applications—potential. Mater Sci Eng 302:37–45
3. Nemcovà A, Skeldon P, Thompson GE, Pacal B (2013) Effect of fluoride on plasma electrolytic oxidation of AZ61 magnesium alloy. Surf Coat Technol 232:827–838
4. Wang L, Chen L, Yan ZC, Wang HL, Peng JZ (2009) Growth and corrosion characteristics of plasma electrolytic oxidation ceramic films formed on AZ31 magnesium alloy. The Chinese journal of Process Engineering 9:592–597
5. Song G, Atrens A (2003) Understanding magnesium corrosion—A framework for improved alloy performance. Adv Eng Mater 5:837–858
6. Rama Krishna L, Somaraju KRC, Sundararajan G (2003) The tribological performance of ultra-hard ceramic composite coatings obtained through microarc oxidation. Surf Coat Technol 484:163–164

7. Nie X, Meletis EI, Jiang JC, Leyland A, Yerokhin AL, Matthews A (2002) Abrasive wear/corrosion properties and TEM analysis of Al_2O_3 coatings fabricated using plasma electrolysis. Surf Coat Technol 149:245–251
8. Snizhko LO, Yerokhin AL, Pilkington A, Gurevina NL, Misnyankin DO, Leyland A, Matthews A (2004) Anodic processes in plasma electrolytic oxidation of aluminium in alkaline solutions. Electrochim Acta 49:2085–2095
9. Cao FH, Lin LY, Zhang Z, Zhang JQ, Cao CN (2008) Environmental friendly plasma electrolytic oxidation of AM60 magnesium alloy and its corrosion re-sistance. Trans Nonferrous Met Soc China 18:240–247
10. Martin J, Melhem A, Shchedrina I, Duchanoy T, Nominè A, Henrion G, Czerwiec T, Belmonte T (2013) Effects of electrical parameters on plasma electrolytic oxidation of aluminium. Surf Coat Technol 221:70–76
11. Ma Y, Nie X, Northwood DO, Hu H (2006) Systematic study of the electrolytic plasma oxidation process on a mg alloy for corrosion protection. Thin Solid Films 494:296–301
12. Guo HL, Huan C, Xing QW, Hua P, Gu LZ, Bin Z, Heon JL, Si ZY (2010) Effect of additives on structure and corrosion resistance of plasma electrolytic oxidation coatings on AZ91D magnesium alloy in phosphate based electrolyte. Surf Coat Technol 205:36–40
13. Sreekanth D, Rameshbabu N, Venkateswarlu K (2012) Effect of various additives on morphology and corrosion behavior of ceramic coatings developed on AZ31 magnesium alloy by plasma electrolytic oxidation. Ceram Int 38:4607–4615
14. Duan H, Yan C, Wang F (2007) Effect of electrolyte additives on performance of plasma electrolytic oxidation films formed on magnesium alloy AZ91D. Electrochim Acta 52:3785–3793
15. Junghoon L, Yonghwan K, Wonsub C (2012) Effect of Ar bubbling during plasma electrolytic oxidation of AZ31B magnesium alloy in silicate electrolyte. Appl Surf Sci 259:454–459
16. Li W, Li C, Wen F (2011) Characterization of plasma electrolytic oxidation films formed on AZ31 magnesium alloys by different voltage parameters. Adv Mat Res 168–170:1203–1208
17. Hussein RO, Northwood DO, Nie X (2012) The influence of pulse timing and current mode on the microstructure and corrosion behaviour of a plasma electrolytic oxidation (PEO) coated AM60B magnesium alloy. J Alloy Compd 541:41–48
18. Bala Srinivasan P, Liang J, Blawert C, Störmer M, Dietzel W (2009) Effect of current density on the microstructure and corrosion behaviour of plasma electrolytic oxidation treated AM50 magnesium alloy. Appl Surf Sci 255:4212–4218
19. Kazanski B, Kossenko A, Zinigrad M, Lugovskoy A (2013) Fluoride ions as modifiers of the oxide layer produced by plasma electrolytic oxidation on AZ91D magnesium alloy. Appl Surf Sci 287:461–466
20. Ma C, Zhang M, Yuan Y, Jing X, Bai X (2012) Tribological behavior of plasma electrolytic oxidation coatings on the surface of Mg-8Li-1Al alloy. Tribol Int 47:62–68
21. Gun KY, Seok LE, Hyuk SD (2014) Influence of voltage waveform on anodic film of AZ91 Mg alloy via plasma electrolytic oxidation: microstructural characteristics and electrochemical responses. J Alloy Compd 586:356–361
22. Ma C, Lu Y, Sun P, Yuan Y, Jing X, Zhang M (2011) Characterization of plasma electrolytic oxidation coatings formed on Mg–Li alloy in an alkaline polyphosphate electrolyte. Surf Coat Technol 206:287–294
23. Seah MP, Briggs D, Seah J (1990) Practical surface analysis, auger and X-ray photoelectron spectroscopy. Wiley & Sons 1:543
24. Shirley DA (1972) High-resolution X-ray photoemission spectrum of the valence bands of gold. Phys Rev B 55:4709
25. Moulder JF, Stickle WF, Sobol PE, Bomben KD, Chastain J (1992) Handbook of X-ray photoelectron spectroscopy. Perkin Elemer Corp, Eden Prairie
26. X-ray photoelectron spectroscopy database 20, Version 3.0, National Institute of Standards and Technology, Gaithersburg
27. http://srdata.nist.gov/XPS
28. Glisenti A, Frasson A, Galenda A, Natile MM (2010) Au/CeO2 supported nanocatalysts: interaction with methanol. Nanoscie Nanotechn Letters 2(3):213–219
29. Natile MM, Tomaello F, Glisenti A (2006) WO3/CeO2 nanocomposite powders; synthesis, characterization, and reactivity. Chem Mater 18:3270–3280
30. Teterin YA, Teterin AY, Lebedev AM, Utkin IO (1998) The XPS spectra of cerium compounds containing oxygen. J Electron Spectr Rel Phenom 88–91:275–279
31. Wang S, Qiao Z, Wang W, Qian Y (2000) XPS studies of nanometer CeO2 thin films deposited by pulse ultrasonic spray pyrolysis. J Alloys Compd 305:121–124
32. Felker DL, Sherwood PMA (2002) Magnesium phosphate *(*Mg3*(*PO4*)*2*)* by XPS. Surf Sci Spectra 9:83–90